



<http://www.scar.ac.cn>

Sciences in Cold and Arid Regions

Volume 8, Issue 2, April, 2016



Citation: Zhang XY, Li ZQ, Zhou P, *et al.*, 2016. Characteristics and source of aerosols at Shiyi Glacier, Qilian Mountains, China. *Sciences in Cold and Arid Regions*, 8(2): 0135–0146. DOI: 10.3724/SP.J.1226.2016.00135.

Characteristics and source of aerosols at Shiyi Glacier, Qilian Mountains, China

XiaoYu Zhang^{1*}, ZhongQin Li^{1,2}, Ping Zhou¹, ShengJie Wang²

1. State Key Laboratory of Cryospheric Sciences, Cold and Arid Regions Environment and Engineering Research Institute; Tianshan Glaciological Station, Chinese Academy of Sciences, Lanzhou, Gansu 730000, China
2. College of Geography and Environment Science, Northwest Normal University, Lanzhou, Gansu 730070, China

*Correspondence to: Ph.D., XiaoYu Zhang, Cold and Arid Regions Environmental and Engineering Research Institute, Chinese Academy of Sciences. No. 320, West Donggang Road, Lanzhou, Gansu 730000, China. Tel: +86-931-4967381; E-mail: zhangxiaoyu@lzb.ac.cn

Received: October 16, 2015

Accepted: December 16, 2015

ABSTRACT

Aerosol samples were collected in the Shiyi Glacier, Qilian Mountains from July 24 to August 19, 2012 and analyzed for major water-soluble ionic species (F^- , Cl^- , NO_2^- , NO_3^- , SO_4^{2-} , Na^+ , NH_4^+ , K^+ , Mg^{2+} and Ca^{2+}) by ion chromatography. SO_4^{2-} and NH_4^+ were the most abundant components of all the anions and cations, with average concentrations of 94.72 and 54.26 neq/m³, respectively, accounting for 34% and 20% of the total water-soluble ions analyzed. These mean ion concentrations were generally comparable with the background conditions in remote sites of the Qilian Mountains, but were much lower than those in certain cities in China. The particles were grouped into two dominant types according to their morphology and EDX signal: Si-rich particles and Fe-rich particles. Backward air mass trajectory analysis suggested that inland cities may contribute some anthropogenic pollution to this glacier, while the arid and semi-arid regions of central Asia were the primary sources of the mineral particles.

Keywords: aerosol; glacier; particles; scanning electron microscopy (SEM)

1 Introduction

Aerosols are an important atmospheric constituent that influences climate, and they are related to human activities (Buseck and Pósfai, 1999). The climatic influence of aerosols is complex. Light scattering by aerosols decreases penetration of solar radiation through the atmosphere and absorption at the surface, increases cloud reflectance, enhances cloud lifetimes, and suppresses precipitation, thereby exerting a cooling influence (Schwartz and Andreae, 1996; Ramanathan *et al.*, 2007). Although a considerable amount of attention has been paid to the radiative properties of aerosols, there are still uncertainties in qualifying their net effect on the global climate, largely due to the high

spatial and temporal variability of aerosol concentrations and properties (Cong *et al.*, 2010). Therefore, better understanding of the various effects of aerosols in the atmosphere requires more detailed information on aerosol chemical and physical properties from diverse geographic locations.

Water-soluble ions comprise a large part of aerosol particles and play an important role in the atmospheric chemistry (Deshmukh and Deb, 2013). It was reported that water-soluble ions such as sulfate, nitrate, and other acid-rain-related pollutants have severe effects on human health (Raizenne *et al.*, 1996).

Individual-particle analysis through scanning electron microscopy and energy dispersive X-ray analysis (SEM-EDX) can provide a great amount of

information on the differences in morphology, elemental composition, and particle density of aerosols to further investigate their potential sources as well as the transport of pollutants, which cannot be obtained through bulk ionic analysis (Paoletti *et al.*, 2002; Reid *et al.*, 2003; Srivastava *et al.*, 2009).

Glaciers of the Qilian Mountains are sensitive indicators of climate change and are natural archives of variations in atmospheric processes. The Qilian Mountains are located at the center of the arid and semi-arid regions of central Asia, in the northeastern edge of the Tibetan Plateau which is connected to the arid region of northwest China. It is the major water source and climate regulation zone of the Hexi Corridor, and also the interaction zone of the Qinghai-Tibet Plateau and Asian dust activities.

Asian dust storms originating from this area as well as from the larger deserts on the planet, which include the Gobi, Taklimakan, and Badain Jaran deserts of Asia, are the primary sources of mobilized desert topsoils that move great distances through the atmosphere each year. Transport and deposition of this dust plays a significant role in the biogeochemical cycles and atmospheric chemistry of the Northern Hemisphere (Arimoto *et al.*, 1996; Griffin, 2007).

The Shiyi Glacier in the Qilian Mountains (Figure 1), with its highest elevation of 4,711 m a.s.l., provides a unique opportunity to improve our understanding of

aerosols transport in the free troposphere, which has potentially significant impacts on regional and global climates, and can deepen our knowledge of physical processes in the cryosphere (Wang *et al.*, 2013).

Studies on atmospheric chemistry have been very limited to date on both temporal and spatial scales in this area. Ion chemistry studies of aerosols have suggested that the atmospheric environment is mainly controlled by natural sources; however, during summer monsoons, man-made pollution emissions cannot be ignored (Wang *et al.*, 2013). Nevertheless, there is no data reported to reflect the air conditions directly. Therefore, in order to obtain updated knowledge of the air conditions, an intensive aerosol sampling experiment was conducted during a scientific expedition to Shiyi Glacier in the Qilian Mountains from July 24 to August 19, 2012.

The purposes of this study were to understand the inorganic ion chemistry properties of the aerosols, determine the elemental compositions and morphological properties of individual aerosol particles, identify their sources of origin, and evaluate the influence of anthropogenic pollutants on the atmosphere over the Qilian Mountains. The 13-day intensive sampling was intended to elucidate the characteristics of aerosols in summer time. This field experiment was the first-ever investigation of inorganic ion chemistry and individual particle analysis of aerosols.

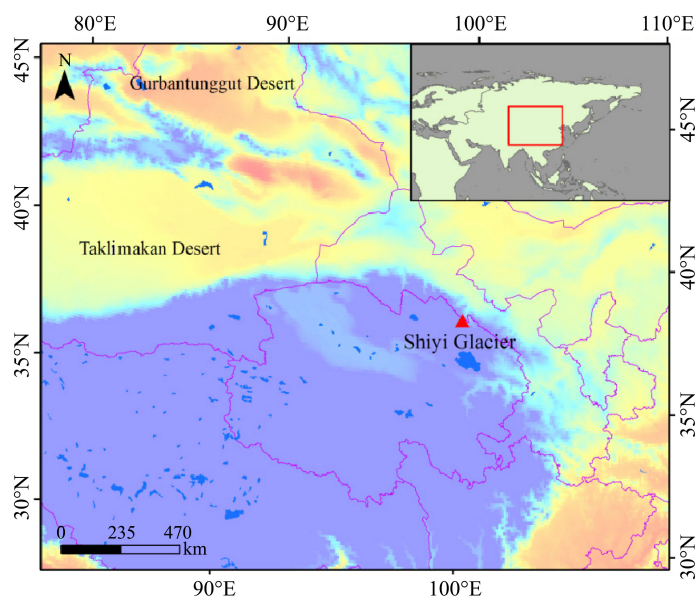


Figure 1 Location map of the Shiyi Glacier with geographic environment

2 Aerosol sampling

Aerosol samples were collected for a 26-day period from July 24 to August 19, 2012. Aerosol samples were recovered on Zefluo Teflon™ filters (2.0- μm pore size, 47-mm diameter; Gelman Sciences) using a 12-V diaphragm pump powered by solar cells. The filters were

loaded in the field and mounted face-down about 1.5 m above the ground surface. Air volume through each filter was measured by an in-line meter and then converted into standard conditions according to the local ambient pressure and temperature. The particle collection efficiency (for particles as small as 0.035 μm) was estimated to be >97% based on the mean flow rate of 1.27

m³/h over the filter (Liu *et al.*, 1984; Zhao *et al.*, 2011).

The sampling period for each aerosol sample was 3–10 h, with samples taken from 09:00 to 18:00 (Beijing time) depending on weather conditions. No samples were collected during rain or snow events. After sampling, the filters were removed from the filter holder and placed in cleaned airtight plastic containers

and stored at 4 °C before analysis. Meteorological parameters, including air temperature, wind speed and direction, precipitation, air pressure, and relative humidity were measured simultaneously by an automatic weather station that was placed near the aerosol sampling site. The actual measured meteorological parameters are summarized in Table 1.

Table 1 Meteorological conditions during the sampling period

Parameters	Units	Mean	Range
Air pressure	hPa	700	70–900
Temperature	°C	7.2	4.7–10.4
Relative humidity	%	71.8	51.3–87.7
Wind speed	m/s	5.5	0.7–12.0

3 Sample analysis

Eight major inorganic ions (Cl⁻, NO₃⁻, SO₄²⁻, Na⁺, NH₄⁺, K⁺, Mg²⁺, and Ca²⁺) of the aerosol samples were analyzed in a class 100 clean room, using a Dionex ion chromatograph (model DX-320; Thermo Fisher Scientific Inc.). To efficiently extract the water-soluble ions from the TeflonTM aerosol filters, each filter was first wetted with 200 μL of ultra-pure methanol and then extracted with 25 mL of deionized water for about 30 min using an ultrasonic water bath device (Sun *et al.*, 1998; Zhao and Li, 2004; Zhao *et al.*, 2011).

The cation chromatography conditions were as follows: a Dionex IonPac CS12A (4mm×250mm) analytical column, 15 mmol/L and 1.0 mL/min methane eluent, and 200 μL sample injected; for anions, an AS11-HC (4mm×250mm) analytical column, 15 mmol/L and 1.0 mL/min NaOH eluent, and 200 μL sample injected (Zhao and Li, 2004).

The average concentrations of 10 laboratory blanks were: Cl⁻ (8.50 ng/g), NO₃⁻ (48.43 ng/g), SO₄²⁻ (6.07 ng/g), Na⁺ (7.76 ng/g), NH₄⁺ (11.71 ng/g), K⁺ (7.11 ng/g), Mg²⁺ (2.36 ng/g), and Ca²⁺ (13.65 ng/g). These were obviously lower than the concentrations detected in the aerosol samples. Mean blank values were subtracted from the sample concentrations and then the sample concentrations were divided by the sample volumes (at standard conditions) of each sample and converted into micrograms per cubic meters, which are listed in Table 2. Detailed sampling methods and analytical techniques of aerosols are described by Zhao and Li (2004) and Zhao *et al.* (2011).

For each membrane, a section of the total filter was cut and mounted onto the electron microprobe stub, and coated with a thin gold film (10 nm) for a higher-quality secondary electron image. The signal of Au in the EDX diagrams appeared at the fixed opposition, and the gold film was too thin to prevent proper identification of the other elemental compositions. In our study, individual particles were analyzed using a

scanning electron microscopy-energy dispersive X-ray spectrometer (SEM-EDX). A section of each filter was cut and mounted onto the electron microprobe stub, and coated with a thin gold film (16 nm) for a higher-quality secondary electron image. The operating conditions were: accelerating voltage in range of 5–10 kV; spectral acquisition time is 60 s. NoranTM System software (Thermo Fisher Scientific Inc.) for energy-dispersive microanalysis was used for the quantitative analysis of individual particles.

4 Results and discussion

4.1 Mass loading of chemical composition of aerosols over Shiyi Glacier

4.1.1 Concentrations of water-soluble inorganic ions in total aerosols

A total of 13 atmospheric aerosol samples were collected during the scientific expedition to Shiyi Glacier. To provide an overview of the chemical composition characteristics, the daily concentrations of the major inorganic ions (F⁻, Cl⁻, NO₂⁻, NO₃⁻, SO₄²⁻, Na⁺, NH₄⁺, K⁺, Mg²⁺, and Ca²⁺) are shown in Table 2. Of all the anions, sulfate was the dominant component, followed by nitrate; of the cations, ammonia had the highest concentration, while the concentrations of chloride and nitrite were much lower than the others.

The concentration of SO₄²⁻ ranged from 17.05 to 315.40 ng/m³, with a mean value of 94.72 ng/m³, while the concentration of NO₃⁻ varied from 55.43 to 8.82 ng/m³, with a mean value of 27.41 ng/m³. The mean concentration of NO₂⁻ was about 3.09 ng/m³ and Cl⁻ was about 6.41 ng/m³. Ammonia and calcium were the most prominent components. The concentration of Ca²⁺ ranged from 13.81 to 133.03 ng/m³ with an average value of 41.32 ng/m³, and the concentration of ammonia varied from 4.06 to 176.13 ng/m³ with an

average value of 54.26 ng/m³; K⁺ and Na⁺ had lower levels of concentration than the other analyzed cationic species, averaging about 6.85–14.49 ng/m³.

The following ion balance calculations are commonly used to evaluate the acid-base balance of aerosol particles:

$$\Sigma^+ = \text{Na}^+/23 + \text{NH}_4^+/18 + \text{K}^+/39 + \text{Mg}^{2+}/12 + \text{Ca}^{2+}/20 \quad (1)$$

$$\Sigma^- = \text{F}^-/19 + \text{Cl}^-/35.5 + \text{NO}_2^-/46 + \text{NO}_3^-/62 + \text{SO}_4^{2-}/48 \quad (2)$$

The ratios of the sum of the equivalent concentrations of cations to anions (Σ^+/Σ^-) were calculated and presented in Table 2. The ion balance expressed by the sum of the concentrations of anion-to-cation is a good indicator to study the acidity of the environment (Verma *et al.*, 2010).

The ratios calculated for all aerosol samples ranged from 0.675 to 2.033. Such variation of ion balance can probably be attributed to the different air masses that arrived at the sampling site, which meant there were different origins with different air conditions.

The Σ^+/Σ^- ratios for the aerosol samples on July 31 and August 3–5 were <1.0, which indicated that these samples were acidic. This was possibly due to the NO₃⁻ and SO₄²⁻ increasing much more than the cations. The Σ^+/Σ^- ratios for the aerosol sample collected on July 29 was 1.02, suggesting that aerosol particles on that day were almost neutral. The ratios of the other samples were >1.0, indicating that they were more alkaline. The total equivalents of anions were plotted against the total equivalents of cations, and the slope of the regression line was slightly lower than unity (Figure 2, slope = 0.97, R² = 0.77), which implied cation deficiencies.

High temperature is probably the primary reason for the volatilization of NH₄⁺ (Khoder and Hassan, 2008). However, the lower temperature over this glacierized region (Table 1) may have contributed to the very low vaporization or volatilization of NH₄⁺ in

our samples. Thus, the cation deficiencies could mostly be attributed to H⁺, which was not counted in Equations (1) and (2) above (Zhao *et al.*, 2011).

Because organic ions are another important constituent of aerosol particles, the lack of organic ions would cause some errors in estimation of the ion balances. Because ions like formate, acetate, and other organic acid ions will contribute to the sum of the equivalent concentration of anions Σ^- , the real values of the Σ^+/Σ^- ratios will become smaller. Therefore, the deviation to the upper side of the theoretical line indicates a deficiency of anions, since bicarbonate, organic ions (formate and acetate), CO₃²⁻, HCO₃⁻, PO₄³⁻ and Br⁻ were not determined in the present study (Khoder and Hassan, 2008).

4.1.2 Correlation between ionic species in aerosols

In order to identify and separate the impacts of various sources, correlation coefficients between the ionic species were calculated and are shown in Table 3. The sum mass concentration of SO₄²⁻, NH₄⁺, NO₃⁻ and Ca²⁺ accounted for about 80% of all the 10 ions measured, and significantly positive correlation coefficients were found between SO₄²⁻ and NH₄⁺ ($r = 0.98$), NO₃⁻ and SO₄²⁻ ($r = 0.79$), and Ca²⁺ and NO₃⁻ ($r = 0.79$).

Querol *et al.* (1998) proposed the presence of (NH₄)₂SO₄·CaSO₄·2H₂O for the NH₄⁺/SO₄²⁻ molar ratio close to 1.0 based on XRD (X-ray diffraction) observations. In the present study, the NH₄⁺/SO₄²⁻ ranged from 0.24 to 0.66, with a mean value of 0.37, and all of the ratios were <1.0, indicating that sulfate may have been present as CaSO₄ and (NH₄)₂SO₄·CaSO₄·2H₂O. Consistent with the observations of previous investigators, NH₄⁺/SO₄²⁻ molar ratios <1.0 could be explained by the combination of sulfate with calcium to form CaSO₄, and with ammonium and calcium to form (NH₄)₂SO₄·CaSO₄·2H₂O (Duan *et al.*, 2003; Khoder and Hassan, 2008).

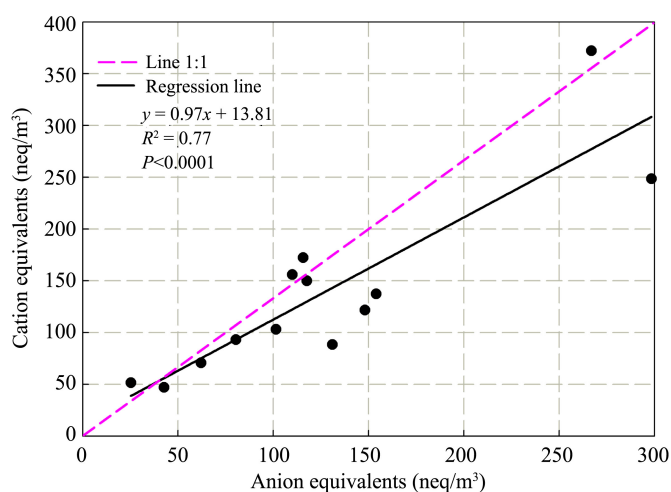


Figure 2 Ion balance of the major water-soluble inorganic ions in the aerosols of Shiyi Glacier, Qilian Mountains

Table 2 Concentrations and ion balance of the water-soluble inorganic ions of Shiyi Glacier

Date	Ion concentrations (neq/m ³)													Σ^{+}	Σ^{-}	Σ^{+}/Σ^{-}
	F ⁻	Cl ⁻	NO ₂ ⁻	NO ₃ ⁻	SO ₄ ²⁻	Na ⁺	NH ₄ ⁺	K ⁺	Mg ²⁺	Ca ²⁺	SO ₄ ²⁻ /Ca ²⁺	NO ₃ ⁻ /SO ₄ ²⁻				
Jul. 24	17.69	6.79	—	9.88	17.05	—	4.06	—	7.34	13.89	1.23	0.58	51.41	25.28	2.03	
Jul. 27	13.71	4.02	—	17.14	35.79	—	23.19	12.79	12.28	13.81	2.59	0.48	70.66	62.08	1.14	
Jul. 28	14.86	3.95	—	22.18	108.91	—	66.64	17.38	14.52	19.11	5.70	0.20	149.90	117.66	1.27	
Jul. 29	13.05	4.29	0.15	18.41	67.15	—	44.35	19.02	14.62	23.45	2.86	0.27	103.06	101.44	1.02	
Jul. 31	15.45	10.45	—	23.69	38.89	—	25.55	41.10	24.14	40.24	0.97	0.61	88.48	131.02	0.68	
Aug. 3	8.75	4.12	—	16.35	92.57	3.94	53.36	14.53	17.91	58.29	1.59	0.18	121.80	148.03	0.82	
Aug. 4	8.89	5.08	—	24.19	99.06	—	62.42	17.15	19.00	55.41	1.79	0.24	137.22	153.96	0.89	
Aug. 5	10.76	7.41	—	55.43	174.80	5.91	99.02	19.80	40.60	133.03	1.31	0.32	248.39	298.36	0.83	
Aug. 9	8.91	1.30	2.82	8.82	25.11	—	14.55	4.57	7.27	16.31	1.54	0.35	46.96	42.70	1.10	
Aug. 14	—	16.57	8.17	55.36	92.23	8.23	42.98	4.38	16.80	43.33	2.13	0.60	172.34	115.71	1.49	
Aug. 15	1.84	7.51	—	47.28	315.40	14.37	176.13	14.08	—	62.30	5.06	0.15	372.03	266.88	1.39	
Aug. 17	6.46	7.31	—	31.58	110.64	4.95	63.18	6.19	9.87	25.77	4.29	0.29	156.00	109.96	1.42	
Aug. 19	7.49	4.51	1.22	26.00	53.82	3.71	29.93	2.87	11.69	32.21	1.67	0.48	93.04	80.41	1.16	
Max	17.69	16.57	8.17	55.43	315.40	14.37	176.13	41.10	40.60	133.03	5.70	0.61	372.03	298.36	2.03	
Min	1.84	1.30	0.15	8.82	17.05	3.71	4.06	2.87	7.27	13.81	0.97	0.15	46.96	25.28	0.68	
Mean	10.66	6.41	3.09	27.41	94.72	6.85	54.26	14.49	16.34	41.32	2.52	0.37	139.33	127.19	1.17	
%	4.00	2.00	1.00	10.00	34.00	2.00	20.00	5.00	6.00	15.00	—	—	0.51	0.46	—	
Max/Min	9.60	12.80	53.10	6.30	18.50	3.90	43.40	14.30	5.60	9.60	5.90	4.10	7.90	11.80	3.00	

Table 3 Inter-species correlation coefficients

	F ⁻	Cl ⁻	NO ₂ ⁻	NO ₃ ⁻	SO ₄ ²⁻	Na ⁺	NH ₄ ⁺	K ⁺	Mg ²⁺	Ca ²⁺
F ⁻	1.00									
Cl ⁻	0.05	1.00								
NO ₂ ⁻	-0.03	0.46	1.00							
NO ₃ ⁻	-0.19	0.61	-0.19	1.00						
SO ₄ ²⁻	-0.05	0.41	-0.15	0.79	1.00					
Na ⁺	-0.33	0.57	0.10	0.75	0.84	1.00				
NH ₄ ⁺	-0.01	0.44	-0.01	0.74	0.98	0.82	1.00			
K ⁺	0.53	0.44	0.03	0.34	0.45	0.22	0.50	1.00		
Mg ²⁺	0.42	0.41	-0.15	0.59	0.40	0.23	0.38	0.68	1.00	
Ca ²⁺	0.13	0.43	-0.15	0.79	0.77	0.62	0.74	0.56	0.84	1.00

To separate anthropogenic sources from natural sources of SO₄²⁻, we calculated the value of the equivalent concentration ratio of SO₄²⁻/Ca²⁺ as described by Ming *et al.* (2007). High values of SO₄²⁻/Ca²⁺ (43.2 and 138.8) near Mount Qomolangma suggested that SO₄²⁻ had primarily anthropogenic sources, while lower value (3.8) suggested primarily dust sources (Ming *et al.*, 2007). The values of SO₄²⁻/Ca²⁺ in our samples ranged from 0.97 to 5.70 (Table 2). This indicated that domestic house heating in winter, industrial coal burning, and other fossil fuel burning were the major potential pollution sources of SO₄²⁻ in this region. This means the SO₄²⁻ in our samples was controlled by both natural processes and anthropogenic sources.

Gaseous NH₃ can be either wet- or dry-deposited, or can neutralize H₂SO₄, HNO₃ and HCl to form ammonium bisulphate (NH₄HSO₄), ammonium nitrate (NH₄NO₃), and ammonium chloride (NH₄Cl) via particle gas formation and gas-to-particle conversion (Baek and Aneja, 2005; Aneja *et al.*, 2009; Ianniello *et al.*, 2011). They are usually formed in these formulae: H₂SO₄+NH₃→NH₄HSO₄; HNO₃ + NH₃ ↔ NH₄NO₃; HCl + NH₃ ↔ NH₄Cl; therefore, some of the NH₄⁺ in this study could also exist as NH₄HSO₄, NH₄NO₃, and NH₄Cl (Ianniello *et al.*, 2011). The formations are significant in summer due to the conversion of gaseous precursors (Wang *et al.*, 2005), while the potential sources for ammonia in the formula are human and agriculture activities such as animal farming, use of fertilizers, and organic decomposition (Sun *et al.*, 1998; Kreutz *et al.*, 2001; Wu *et al.*, 2006; Verma *et al.*, 2010).

Nitrogen oxides emissions from mobile sources are an important contributor to NO₃⁻ in the atmosphere. Therefore, the mass ratio of NO₃⁻/SO₄²⁻ has been used as an indicator of the relative importance of stationary versus mobile sources of sulfur and nitrogen in the atmosphere (Arimoto *et al.*, 1996; Khoder and Hassan 2008). Arimoto *et al.* (1996) ascribed a high NO₃⁻/SO₄²⁻ mass ratio to the predominance of mobile sources over stationary sources of pollutants. In the

present study, the average mass ratios of NO₃⁻/SO₄²⁻ were 0.37 on average, relatively similar to that found in some cities in China, such as Shanghai (0.43; Yao *et al.*, 2002), Qingdao (0.35; Hu *et al.*, 2002). This was slightly higher than those reported in Taiwan (0.2; Fang *et al.*, 2002) and Guiyang (0.13; Xiao and Liu, 2004), and lower than those found in Beijing during 2001–2003 (0.71; Wang *et al.*, 2005) and Shanghai in 2006 (0.83; Wang *et al.*, 2006). Generally, the mass ratio of NO₃⁻/SO₄²⁻ in the aerosols of Shiyi Glacier was <1.0, suggesting that stationary source emissions were more predominant.

NO₃⁻ is the most of the reaction product of NO_x emission, while the NO_x emission is mainly due to fossil fuel combustion and biomass burning (Wang *et al.*, 2006; Wu *et al.*, 2006). Under an alkaline atmospheric environment, gaseous HNO₃ formed by the oxidation of NO_x can be absorbed on the surface of mineral particles and reacted to form salts (Mamane and Gottlieb, 1992). This may be the reason why NO₃⁻ has significant correlations with Na⁺, NH₄⁺ and Ca²⁺ ($r = 0.75, 0.74, \text{ and } 0.79$, respectively). Previous studies found that automobile exhaust is a major contributor of NO₃⁻ (Arimoto *et al.*, 1996; Wang *et al.*, 2005, 2006; Bhaskar *et al.*, 2010). Glacio-chemical investigation from the Belukha Glacier (Olivier *et al.*, 2003) also pointed out that increased nitrates resulted from the growth of traffic and the associated rise of the emission of precursor gases NO_x. Therefore, the higher content of NO₃⁻ in our study was likely related to anthropogenic pollutions, and traffic emissions from Qilian County may also be a potential source.

Significant correlations with Ca²⁺, Na⁺, SO₄²⁻ and NO₃⁻ suggest that there are some other compounds originating from desert dust, existing as Na₂SO₄, NaNO₃ and Ca(NO₃)₂. Calcium is usually rich in desert and loess soils, and even in atmospheric aerosol particles collected from the desert and loess areas, Ca²⁺ was always accepted as a proxy for dust in past studies of snow and ice chemistry (Mayewski *et al.*, 1993; Wolff, 1996; Zhang and Edwards, 2011). Previous studies over the Tianshan Mountains found that the

surrounding desert and arid regions were usually considered to be the primary sources of Ca^{2+} (Williams *et al.*, 1992; Sun *et al.*, 1998; Aizen *et al.*, 2004; Zhang *et al.*, 2008; Zhang *et al.*, 2012). Okada and Kai (2004) also found that the calcium-rich mineral particles in deserts usually present as CaCO_3 , CaSO_4 , and internal mixtures of CaCO_3 and CaSO_4 or silicates. However, in this study the potential existence of $\text{Ca}(\text{NO}_3)_2$ gave us a new revelation, that is, human activity has already affected this region by the use of chemical fertilizers, because calcium nitrate is a typical fast-acting fertilizer material used in agriculture. It is also used in the electronics industry for coating cathodes.

Halite (NaCl) particles were commonly detected in aerosol particles collected over the Taklimakan Desert (Okada and Kai, 2004). Wake *et al.* (1990) and Sun *et al.* (1998) also pointed out that Na^+ and Cl^- in the Tianshan Mountains represent an input of Na^+ and Cl^- rich dust originating from the extensive evaporate deposits in the arid regions surrounding these mountain ranges.

Potassium is also probably derived from the evaporation of insecticides, chemical fertilizers, and dust, because it has higher correlations with F^- and SO_4^{2-} ($r = 0.53$ and 0.45 , respectively).

4.1.3 Comparison with data of the other areas

In our study, mean ion concentrations of the aerosol samples were ordered as $\text{SO}_4^{2-} > \text{NH}_4^+ > \text{Ca}^{2+} > \text{NO}_3^- > \text{Mg}^{2+} > \text{K}^+ > \text{F}^- > \text{Na}^+ > \text{Cl}^- > \text{NO}_2^-$. These mean ion concentrations of the Shiyi Glacier were generally comparable with the background conditions in remote sites in the Qilian Mountains and the Tianshan Bogda Glacier, except that SO_4^{2-} and Ca^{2+} were slightly higher, and the ion concentrations were much lower than those in cities such as Beijing of China and Raipur of India (Table 4).

4.2 Individual particles analysis

The particles were grouped into two dominant types according to their morphology and EDX signal (Table 5). Figure 3 shows the typical individual particles loaded on the filters at different magnifications. The distinct characteristics and possible origins of each group are described in detail as follows.

4.2.1 Si-rich particles

Mineral particles, comprising silicates (Na_2SiO_3 , $\text{CaMg}_3\text{Si}_4\text{O}_{12}$, $\text{K}_2\text{Al}_2\text{Si}_6\text{O}_{16}$, $\text{Al}_2(\text{OH})_4\text{Si}_2\text{O}_5$), quartz (SiO_2), feldspars (KAlSi_3O_8 , $\text{NaAlSi}_3\text{O}_8$, $\text{CaAl}_2\text{Si}_2\text{O}_8$), gypsum (CaSO_4), calcite (CaCO_3), and pyroxene (Ca , Mg , Fe , Al)₂(Si , Al)₂ O_6 , *etc.*, were the richest particles over this region. The sizes of the mineral particles generally ranged from 0.6 to 14.1 μm . Most of these

particles had irregular shapes (Figure 3), suggesting that they were from natural sources. Particles containing predominantly silicon were classified as quartz (SiO_2), with the irregular shapes shown in Figures 3a,b,d. As an important constituent of many rock types and dust, quartz is almost ubiquitous on land areas.

In our study, particles containing Si were the major composition, with an average abundance of 38.3%. These particles can mainly be attributed to the surrounding dust sources or aeolian dispersion of soil particles, which originated from local deserts or through long-range transport from the west. This was similar to the results of aerosols collected from the high Himalayas (Cong *et al.*, 2010).

About 11.5% of the particles were identified with high amounts of Ca. These particles could be classified into three types in theory: calcium sulfates characterized by high and approximately equal amounts of Ca and S, and calcium carbonates and calcium nitrates characterized by only relatively high X-ray intensities of Ca. The primary natural source of calcium sulfate is gypsum, a typical mineral in the earth crust but generally much less abundant than CaCO_3 (Gao *et al.*, 2007). Since the lighter elements such as C, N, and O are very difficult to quantify from EDS spectra, calcium nitrate and carbonate cannot be distinguished in an automated analysis, which is why calcium sulfate is easily identified.

4.2.2 Fe-rich particles

Fe-rich particles are considered to be oxides (hematite, magnetite) or oxyhydroxides (goethite) (Cong *et al.*, 2010). Fe-rich particles accounted for 27.2% of the findings in the Shiyi Glacier. Besides soil dispersion, Fe-rich particles can also be produced by coal-fired boilers, metal industries, and power plants. Fe-rich particles emanated from a high-temperature furnace usually show a spherical shape. However, Fe particles in this study had irregular (non-spherical) morphology (Figure 3c), and were thus identified as being of natural origin.

There were also some very small spherical-shaped particles with smooth edges and surfaces, shown in Figures 3a,c; these were likely emitted by a high-temperature process. They may have originated from the steel industry or from coal combustion. These unrecognized particles could contain organic particles with light elements (such as C, N, and O) or biological particles.

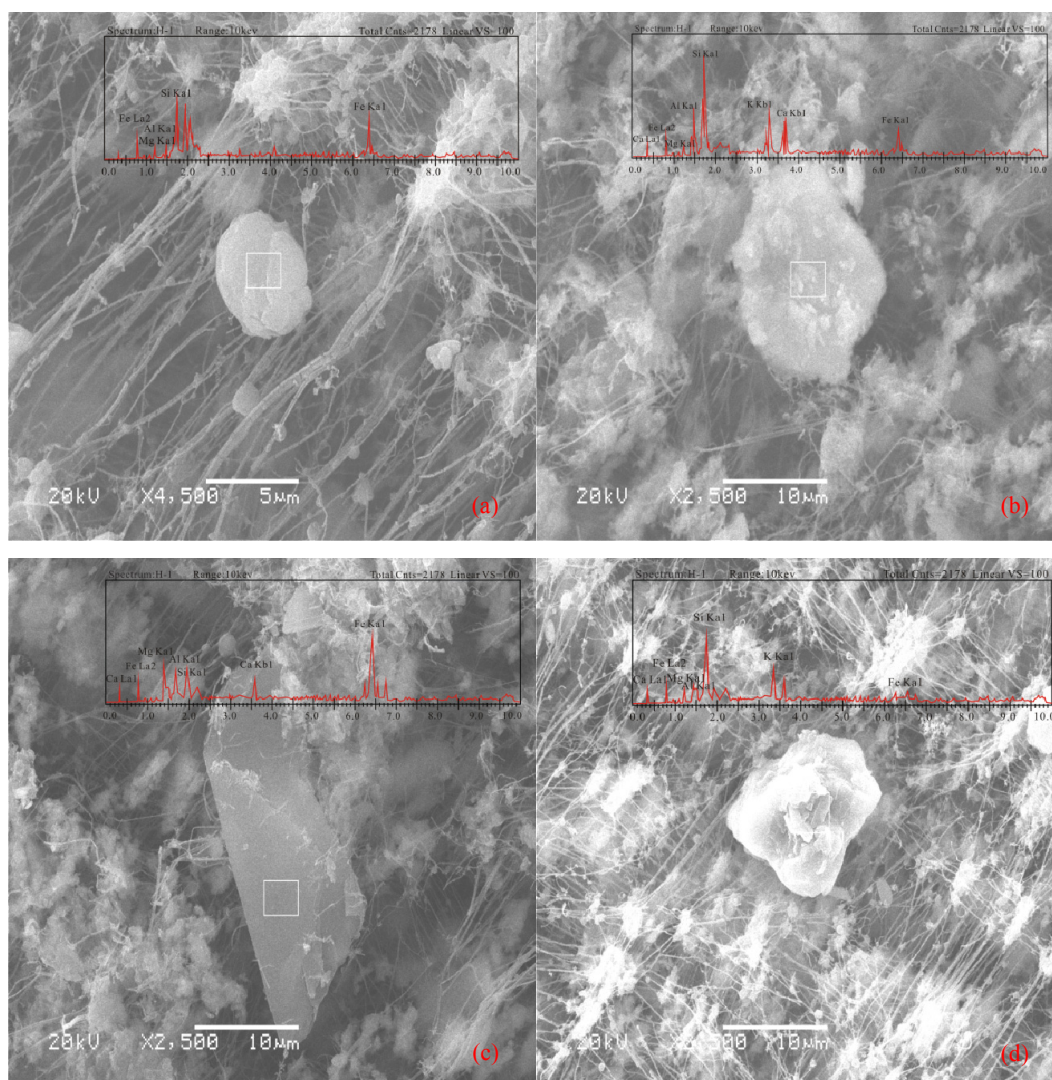
In summary, most of the large particles detected over the Shiyi Glacier were probably from natural mineral dust, while very small particles may have been emitted by anthropogenic activities. This suggests that both natural processes and anthropogenic pollution were the aerosol sources over this glacierized site during the sampling period.

Table 4 Water-soluble inorganic ions ($\mu\text{g}/\text{m}^3$) of aerosols at different sites all over the world

Sampling place	Study period	Cl^-	NO_3^-	SO_4^{2-}	Na^+	NH_4^+	K^+	Mg^{2+}	Ca^{2+}	References
Shiyi Glacier	Jul. 2012–Aug. 2012	0.23	1.70	4.55	0.16	0.98	0.56	0.20	0.83	This study
Raipur, India	Jul. 2009–Jun. 2010	3.23	5.63	–	1.75	5.18	0.87	0.80	2.53	Deshmukh <i>et al.</i> (2013)
Beijing, China	2001–2003	2.69	21.10	24.80	1.60	11.90	1.74	2.04	9.05	Wang <i>et al.</i> (2005)
Ishikawa, Japan	2001–2003	3.10	11.50	17.10	0.60	8.70	1.60	0.20	1.60	Sun <i>et al.</i> (2004)
Bogda Glacier, Tianshan Mts.	Jul. 2009–Aug. 2009	2.77	1.77	–	1.86	1.31	0.12	0.23	0.25	Zhao <i>et al.</i> (2011)
Qilian Mountains	Jul. 2010–Jul. 2011	0.05	0.56	0.86	0.11	0.09	0.13	0.01	0.28	Wang <i>et al.</i> (2013)

Table 5 Individual particle types determined by clustering and their relative abundance

Cluster	Type	Cluster number	Counts (s)	Atomic (%)	Relative weight (%)					
					Si	Mg	Al	Ca	Fe	K
A	Si-rich	C1	11.10	64.54	55.85	8.73	5.16	–	30.26	–
		C2	34.65	41.68	34.62	1.71	12.27	15.80	13.74	21.87
		C4	21.94	60.84	53.04	2.50	5.33	7.01	10.63	21.49
B	Fe-rich	C3	2.44	37.59	9.72	13.03	11.61	11.68	53.96	–

**Figure 3** SEM images of typical aerosol particles. (a), (b), (d): Si-rich particles; (c): Fe-rich particles

4.2.3 Particle shapes indicated by particle circularity

We used particle circularity as the shape parameter to characterize the degree of shape complexity of the particles. The circularity was defined as:

$$C = L^2/(4\pi A) \quad (3)$$

where C is circularity (non-dimensional), L is particle perimeter (μm), and A is the two-dimensional area of the particle in the SEM image (μm^2) (Gao *et al.*, 2007).

A circle has a circularity of 1.0, and a square has a circularity of 1.27. As the shape gets more complex, the circularity value increases. The circularity of the Si-rich type of dust particles (Figures 3a,b,d) ranged from 2.9 to 4.4, with a mean value of 3.77, suggesting the non-spherical nature of dust particles over the region.

4.3 Relationships with air mass transport

The Hybrid Single-Particle Lagrangian Integrated Trajectory (HYSPPLIT) model of the NOAA Air Resources Laboratory has been widely used in previous studies (*e.g.*, Ming *et al.*, 2007; Cong *et al.*, 2010). We used this model to simulate five-day backward air trajectories with a daily resolution to identify potential transport pathways and possible source regions of the aerosols at the Shiyi Glacier. Figure 4 presents the daily backward trajectories terminated at the sampling site (38.21°N, 99.88°E; 4,637 m a.s.l.) during the sampling periods. Most of the air masses were transported from the west, northwest, and south. Combined with the ion concentrations listed in Table 2, air masses arriving at the sampling site could be classified into three types:

1) The air masses which arrived on August 3, 15, and 19 originated from or were transported through the arid regions of Kazakhstan, Kyrgyzstan, Uzbekistan, and the northern region of the Taklimakan Desert. They then passed through the urban area of Yumen City, Dunhuang City, Qinghai Lake, and Qilian County, which may have resulted in the input of desert dust and some anthropogenic pollution. These air masses caused the higher concentrations of cations. Also, the concentrations of SO_4^{2-} , NO_3^- , and NH_4^+ were very high.

2) The air masses which arrived on July 24 and July 31 represented the short-range aerosol transport of air masses originating from the western edge of the Badan Jaran Desert. They passed through the north slope of the Qilian Mountains and arrived at the glacier. The relatively lower concentrations of SO_4^{2-} , NO_2^- , NO_3^- , and NH_4^+ at the Shiyi Glacier may be attributed to these cleaner air masses.

3) The air masses which arrived on July 27 and July 29, and August 4 and 5 represented the short-range aerosol transport of air masses originating from the south, specifically the Sichuan Hengduan Mountains. They crossed over two other provinces (Gansu and

Qinghai) and finally reached our sampling site.

Our backward air mass trajectory analysis suggested that inland cities may have contributed some anthropogenic pollution to this glacier, while the arid and semi-arid regions of central Asia were the primary sources of the mineral particles.

5 Conclusions

Intensive aerosol sampling experiments were conducted from July 24 to August 19, 2012, providing the first-ever information about the atmosphere over the Shiyi Glacier in the Qilian Mountains. Inorganic ion chemistry and individual particle characteristics of the aerosols were analyzed through ion chromatography and SEM-EDX, respectively.

The results showed that SO_4^{2-} and NH_4^+ were the most abundant components of all the anions and cations, respectively. Of all the anions, sulfate was the dominant component, followed by nitrate. Ammonia had the highest concentration of the cations, while concentrations of chloride and nitrite were much lower than the others.

The relationship between the eight inorganic ion species and their origins indicated that domestic house heating in winter, industrial coal burning, and burning of other fossil fuels were the potential pollution sources of SO_4^{2-} in this region. The SO_4^{2-} in our samples was controlled by both natural processes and anthropogenic sources.

The mass ratio of $\text{NO}_3^-/\text{SO}_4^{2-}$ in the aerosols of the Shiyi Glacier was <1.0 , suggesting that the stationary source emissions were more predominant, while the potential existence of $\text{Ca}(\text{NO}_3)_2$ suggested that human activity has already affected this region by the use of chemical fertilizers.

Based on morphology, elemental compositions, and EDX signal, the particles were grouped into two dominant types: Si-rich particles and Fe-rich particles. Most of the large detected particles over this region were probably from natural mineral dust, while very small particles may have been emitted by anthropogenic activities. This suggests that both natural processes and anthropogenic pollution were the aerosol sources over the Shiyi Glacier during the sampling period.

Acknowledgments:

This research was jointly supported by the National Natural Science Foundation of China (Nos. 41201065, 41121001, 41261017, 41171057, 41161012); Funds for Creative Research Groups of China (No. 41121001), the Foundation for Excellent Youth Scholars of CAREERI, CAS (No. 51Y251B51); the SKLCS Foundation (No. SKLCSZZ-2012-01-01); the National Basic Research Program of China (Nos. 2010CB951003, 2010CB951404), and the Knowledge

Innovation Project of the Chinese Academy of Sciences (No. KZCX2-EW-311). We would like to thank WenBin Wang, MingYing Xia, YuanYang She,

XuLiang Li, and Shuang Jin for the sampling, and YuMan Zhu, QiuFang Bao, and YaPing Liu for the chemical analyses.

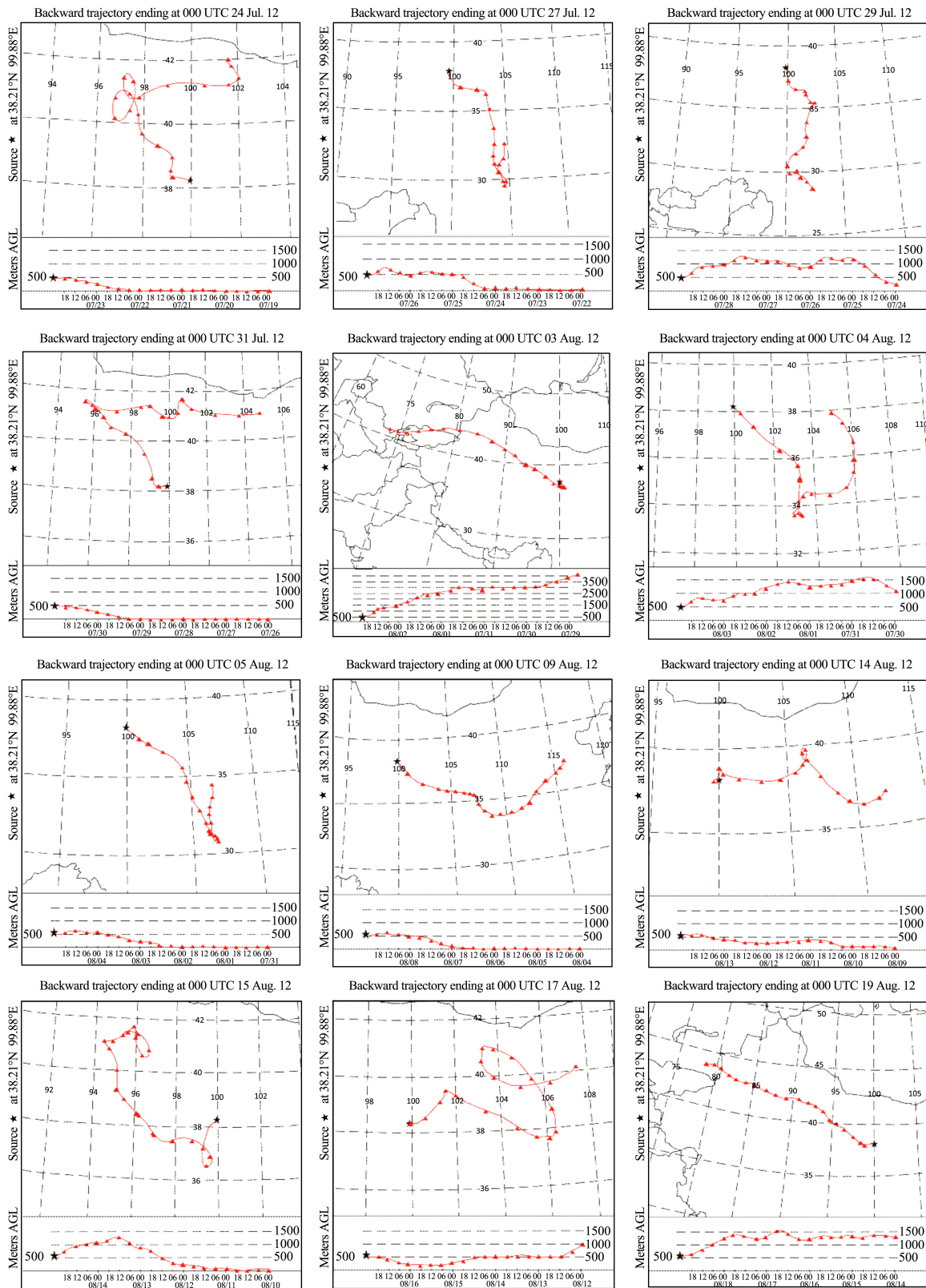


Figure 4 Daily backward trajectories arriving at the sampling site (38.21°N, 99.88°E; 4,637 m a.s.l.)

References:

- Aizen VB, Aizen EM, Melack JM, *et al.*, 2004. Association between atmospheric circulation patterns and firn-ice core records from the Inilchek glacierized area, Central Tien Shan, Asia. *Journal of Geophysical Research*, 109(D08304). DOI: 10.1029/2003JD003894.
- Aneja VP, Schlesinger WH, Erisman JW, 2009. Effects of agriculture upon the air quality and climate: research, policy, and regulations. *Environmental Science & Technology*, 43: 4234–4240.
- Arimoto R, Duce RA, Savoie DL, *et al.*, 1996. Relationships among aerosol constituents from Asia and the North Pacific during Pem-West A. *Journal of Geophysical Research*, 101: 2011–2023.
- Baek BH, Aneja VP, 2005. Observation based analysis for the determination of equilibrium time constant between ammonia, acid gases, and fine particles. *International Journal of Environment and Pollution*, 23(3): 239–247.
- Bhaskar BV, Jeba Rajasekhar RV, Muthusubramanian P, *et al.*, 2010. Ionic and heavy metal composition of respirable particulate in Madurai, India. *Environmental Monitoring and Assessment*, 164: 323–336.
- Buseck PR, Pósfai M, 1999. Airborne minerals and related aerosol particles: Effects on climate and the environment. *Proceedings of the National Academy of Sciences*, 96(7): 3372–3379.
- Cong ZY, Kang SC, Dong SP, *et al.*, 2010. Elemental and individual particle analysis of atmospheric aerosols from high Himalayas. *Environmental Monitoring and Assessment*, 160: 323–335.
- Deshmukh DK, Deb MK, Suzuki Y, *et al.*, 2013. Water-soluble ionic composition of PM_{2.5–10} and PM_{2.5} aerosols in the lower troposphere. *Air Quality Atmosphere and Health*, 6: 95–110.
- Duan FK, Liu XD, He KB, *et al.*, 2003. Atmospheric aerosol concentration level and chemical characteristics of water-soluble species in wintertime in Beijing, China. *Journal of Environmental Monitoring*, 5: 569–573.
- Fang G, Chang C, Wu Y, *et al.*, 2002. Ambient suspended particulate matters and related chemical species study in central Taiwan, Taichung during 1998–2001. *Atmospheric Environment*, 36: 1921–1928.
- Gao Y, Anderson J, Hua X, 2007. Dust characteristics over the North Pacific observed through shipboard measurements during the ACE-Asia experiment. *Atmospheric Environment*, 41: 7907–7922.
- Griffin DW, 2007. Atmospheric movement of microorganisms in clouds of desert dust and implications for human health. *Microbiology Reviews*, 20(3): 459–477. DOI: 10.1128/CMR.00039-06Clin.
- Hu M, He L, Zhang Y, *et al.*, 2002. Seasonal variation of ionic species in fine particles at Qingdao, China. *Atmospheric Environment*, 36: 5853–5859.
- Ianniello A, Spataro F, Esposito G, *et al.*, 2011. Chemical characteristics of inorganic ammonium salts in PM_{2.5} in the atmosphere of Beijing (China). *Atmospheric Chemistry and Physics*, 11: 10803–10822.
- Khoder MI, Hassan SK, 2008. Weekday/weekend differences in ambient aerosol level and chemical characteristics of water-soluble components in the city centre. *Atmospheric Environment*, 42: 7483–7493.
- Kreutz KJ, Aizen VB, Cecil LD, *et al.*, 2001. Oxygen isotopic and soluble ionic composition of a shallow firn core, Inilchek glacier, central Tien Shan. *Journal of Glaciology*, 47(159): 548–554.
- Liu BYH, Pui DYH, Rubow KL, 1984. Characteristics of air sampling filter media. Aerosols in the mining and industrial work environments. In: Marple VA, Liu BYH (eds.). *Instrumentation*, Vol. 3. Newton, MA: Butterworth-Heinemann, pp. 989–1038.
- Mamane Y, Gottlieb J, 1992. Nitrate formation on sea-salt and mineral particles—a single particle approach. *Atmospheric Environment*, 26: 1763–1769. DOI: 10.1126/science.261.5118.195.
- Mayewski PA, Meeker LD, Whitlow S, *et al.*, 1993. The atmosphere during the Younger Dryas. *Science*, 261: 192–197.
- Ming J, Zhang D, Kang S, *et al.*, 2007. Aerosol and fresh snow chemistry in the East Rongbuk Glacier on the northern slope of Mt. Qomolangma (Everest). *Journal of Geophysical Research*, 112(D15): D15307. DOI: 10.1029/2007JD008618.
- Okada K, Kai KJ, 2004. Atmospheric mineral particles collected at Qira in the Taklamakan Desert, China. *Atmospheric Environment*, 38: 6927–6935.
- Olivier S, Schwikowski M, Brütsch S, *et al.*, 2003. Glaciochemical investigation of an ice core from Belukha glacier, Siberian Altai. *Geophysical Research Letters*, 30(19): 2019. DOI: 10.1029/2003GL018290.
- Paoletti L, De Berardis B, Diociaiuti M, 2002. Physico-chemical characterisation of the inhalable particulate matter (PM₁₀) in an urban area: An analysis of the seasonal trend. *Science of the Total Environment*, 292(3): 265–275.
- Querol X, Alastuey A, Puigercus JA, *et al.*, 1998. Seasonal evolution of suspended particles around a large coal-fired power station: chemical characterization. *Atmospheric Environment*, 32: 719–731.
- Raizenne M, Neas LM, Damokosh AL, *et al.*, 1996. The effects of acid aerosols on North American children: pulmonary function. *Environment Health Perspectives*, 104: 506–514.
- Ramanathan V, Ramana MV, Roberts G, *et al.*, 2007. Warming trends in Asia amplified by brown cloud solar absorption. *Nature*, 448: 575–578. DOI: 10.1038/nature06019.
- Reid EA, Reid JS, Meier MM, *et al.*, 2003. Characterization of African dust transport to Puerto Rico by individual particle and size segregated bulk analysis. *Journal of Geophysical Research*, 108(D19): 8591. DOI: 10.1029/2002JD002935.
- Schwartz SE, Andreae MO, 1996. Uncertainty in climate change caused by aerosols. *Science*, 272(5265): 1121–1122. DOI: 10.1126/science.272.5265.1121.
- Srivastava A, Jain V, Srivastava A, 2009. SEM-EDX analysis of various sizes aerosols in Delhi India. *Environmental Monitoring and Assessment*, 150: 405–416.
- Sun J, Qin D, Mayewski PA, *et al.*, 1998. Soluble species in aerosol and snow and their relationship at Glacier 1, Tien Shan, China. *Journal of Geophysical Research*, 103(D21): 28021–28028.
- Sun Y, Zhuang G, Wang Y, *et al.*, 2004. The air-born particulate pollution in Beijing—concentration, composition, distribution and sources. *Atmospheric Environment*, 38: 5991–6004.
- Verma SK, Deb MK, Suzuki Y, *et al.*, 2010. Ion chemistry and source identification of coarse and fine aerosols in an urban area of eastern central India. *Atmospheric Environment*, 95: 65–76.
- Wake CP, Mayewski PA, *et al.*, 1990. A review of Central Asian glaciochemical data. *Annals of Glaciology*, 14: 301–306.

- Wang Y, Zhuang G, Tang A, *et al.*, 2005. The ion chemistry and the source of PM_{2.5} aerosol in Beijing. *Atmospheric Environment*, 39(21): 3771–3784.
- Wang Y, Zhuang G, Zhang X, *et al.*, 2006. The ion chemistry, seasonal cycle, and sources of PM_{2.5} and TSP aerosol in Shanghai. *Atmospheric Environment*, 40: 2935–2952.
- Wang ZB, Xu JZ, Yu GM, *et al.*, 2013. The characteristics of soluble ions in PM_{2.5} aerosol over the Qilian Shan Station of glaciology and ecologic environment. *Journal of Glaciology and Geocryology*, 35(2): 336–344.
- Williams MW, Tonnessen KA, Melack JM, *et al.*, 1992. Sources and spatial variation of the chemical composition of snow in Tien Shan, China. *Annals of Glaciology*, 16: 25–37.
- Wolff EW, 1996. The record of aerosol deposited species in ice core, and problem of interpretation. In: Wolff EW, Bales R (eds.). *Chemical Exchange between the Atmosphere and Polar Snow*. New York: Springer, pp. 1–17.
- Wu D, Tie X, Deng X, 2006. Chemical characterizations of soluble aerosols in southern China. *Chemosphere*, 64: 749–757.
- Xiao H, Liu C, 2004. Chemical characteristics of water soluble components in TSP over Guiyang, SW China, 2003. *Atmospheric Environment*, 38: 6297–6306.
- Yao X, Chan CK, Fang M, *et al.*, 2002. The water-soluble ionic composition of PM_{2.5} in Shanghai and Beijing, China. *Atmospheric Environment*, 36: 4223–4234.
- Zhang K, Li Z, Wang F, *et al.*, 2008. Soluble mineral dusts in aerosol and surface snow on the Glacier No. 1 at the headwaters of Ürümqi River, east Tianshan Mountains: Characteristics and their interrelation—taking calcium and magnesium as examples. *Journal of Glaciology and Geocryology*, 31(1): 113–118.
- Zhang XY, Edwards R, 2011. Anthropogenic sulfate and nitrate signals in snow from Glacier of Mt. Bogda, Eastern Tianshan. *Journal of Earth Science*, 22(4): 490–502.
- Zhang XY, Li ZQ, Wang FT, *et al.*, 2012. Chemistry and environmental significance of snow on Glacier No. 72, Mt. Tumor, Tianshan Mountains, Central Asia. *Scientia Geographica Sinica*, 32(5): 636–641.
- Zhao SH, Li ZQ, Zhou P, 2011. Ion chemistry and individual particle analysis of atmospheric aerosols over Mt. Bogda of eastern Tianshan Mountains, Central Asia. *Environmental Monitoring and Assessment*, 180: 409–426.
- Zhao ZP, Li ZQ, 2004. Determination of soluble ions in atmospheric aerosol by ion chromatography. *Modern Scientific Instrument*, 5: 46–49.